POLITECNICO DI TORINO
Repository ISTITUZIONALE

A Sustainable, Bidirectional Soft Pneumatic Actuator for Robotic Systems

*Original*
A Sustainable, Bidirectional Soft Pneumatic Actuator for Robotic Systems / Duretto, S., Colucci, G., Tagliavini, L., Botta, A., Toccaceli, L., Quaglia, G.. - ELETTRONICO. - 1:(2025), pp. 549-558. (3rd International Conference of IFToMM for SDG (I4SDG2025) Villa San Giovanni (ITA) 9-12 June 2025) [10.1007/978-3-031-91151-4_60].

*Availability:*
This version is available at: 11583/3002814 since: 2025-09-05T07:47:12Z

*Publisher:*
Springer

*Published*
DOI:10.1007/978-3-031-91151-4_60

*Terms of use:*

This article is made available under terms and conditions as specified in the corresponding bibliographic description in the repository

*Publisher copyright*
Springer postprint/Author's Accepted Manuscript

This version of the article has been accepted for publication, after peer review (when applicable) and is subject to Springer Nature's AM terms of use, but is not the Version of Record and does not reflect post-acceptance improvements, or any corrections. The Version of Record is available online at: http://dx.doi.org/10.1007/978-3-031-91151-4_60

(Article begins on next page)

26 November 2026

# A Sustainable, Bidirectional Soft Pneumatic Actuator for Robotic Systems

Simone Duretto(✉), Giovanni Colucci, Luigi Tagliavini, Andrea Botta, Lorenzo Toccaceli, and Giuseppe Quaglia

Department of Mechanical and Aerospace Engineering, Politecnico di Torino, Corso Duca degli Abruzzi 24, 10129 Torino, Italy
{simone.duretto,giovanni_colucci,luigi.tagliavini,andrea.botta, lorenzo.toccaceli,giuseppe.quaglia}@polito.it

**Abstract.** BiSoft.Q is a bidirectional Soft Pneumatic Actuator that offers unique advantages such as compliance, lightness, no friction, low hysteresis, and low activation pressure. This paper investigates the air consumption of BiSoft.Q for its application in robotic systems. To estimate air consumption, a theoretical model is developed and then experimentally validated. The proposed model provides a foundation for future research on energy efficiency optimization of this promising actuator.

**Keywords:** SDG12 · Soft Actuator · Soft Robotics · Sustainability · Service Robot.

## 1 Introduction

Soft Pneumatic Actuators (SPAs) are widely appreciated for their high force-to-mass ratio and compliance. However, SPAs always present a dead volume, defined as the volume that needs to be pressurized although not contributing to the generation of force [2]. Therefore, for single chamber SPAs, like McKibben muscle and PPAM, various strategies have been proposed to reduce dead volume and thus energy consumption. These include filling the dead volume with solid, granular, or liquid fillers [3,5].

In recent times, the authors designed a novel SPA, BiSoft.Q, which implements two antagonistic chambers to produce a bidirectional and linear motion [1]. As with all SPAs, BiSoft.Q is compliant and lightweight, but with even lower hysteresis and friction than PPAMs and a low activation pressure. Moreover, being a pneumatic actuator, BiSoft.Q can hold its position under load without consuming additional energy, as opposed to electric actuators. Finally, its two chambers are suitable for implementing exhausted air recirculation strategies similar to those presented in [4,6].

These peculiarities make BiSoft.Q an interesting choice for application in robotic systems, in which the reduction of moving masses, as well as the reduction of the energy necessary to power the system, are a major concern. For instance, Fig. 1(a) shows the application of BiSoft.Q in a fin-ray gripper, where the bi-directionality of the actuator is exploited to perform inner and outer grasping and its compliance is used to compensate centering errors, while at the same time achieving a significant reduction of the end-effector's mass with respect to a standard one.

However, similarly to conventional SPAs, BiSoft.Q has significant dead volumes that limit its energy efficiency. Therefore, the aim of this study is to characterize BiSoft.Q's air consumption, both theoretically and experimentally, in order to provide a foundation for future studies on the energy efficiency optimization of the actuator.

## 2 BiSoft.Q Concept and Modeling

BiSoft.Q exploits two antagonistic chambers that can be pressurized independently to generate a bidirectional, linear motion. These chambers are defined by two deformable membranes (Fig. 1(c)): the outer one is a pleated membrane, while the inner one is a bellows. As shown in Fig. 1(b), the pressurization of the outer chamber makes the actuator contract and exert a pulling force. Instead, the pressurization of the inner chamber results in the extension of the actuator and the exertion of a pushing force.

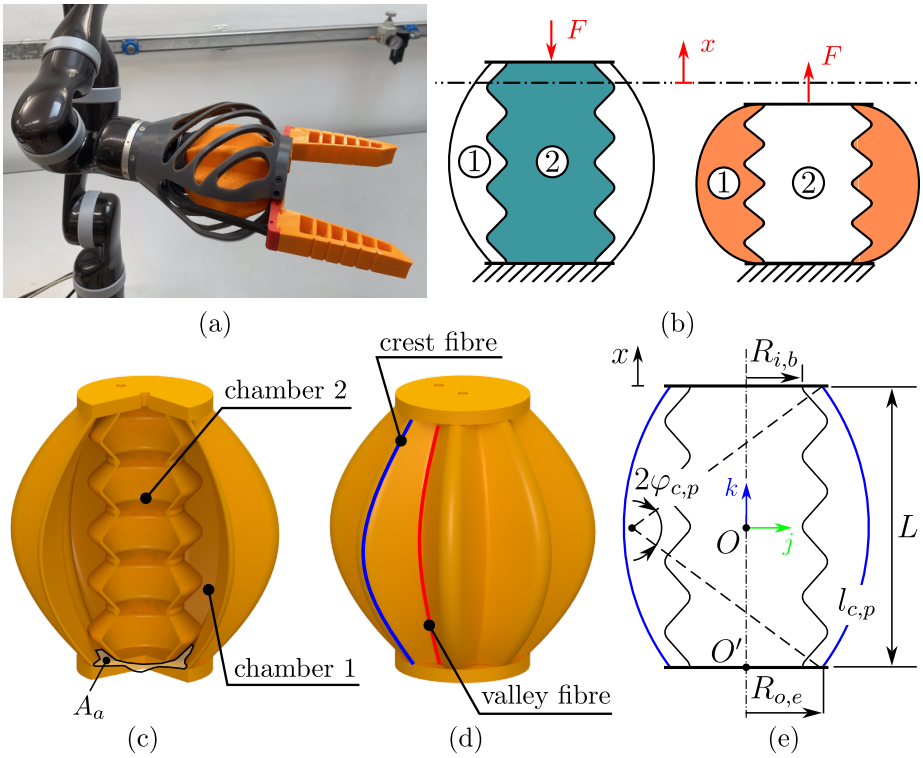



**Fig. 1.** (a) Application of BiSoft.Q in a fin-ray gripper. (b) Working modes of the actuator (the pressurized chamber is highlighted). $x = 0$ is the configuration at rest, while $F$ is the external force that counterbalances the one generated by the actuator. (c) Identification of the antagonistic chambers of BiSoft.Q. (d) Definition of crest and valley fibres of the pleated membrane. (e) Longitudinal cross section passing through the crest fibre of the pleated membrane.

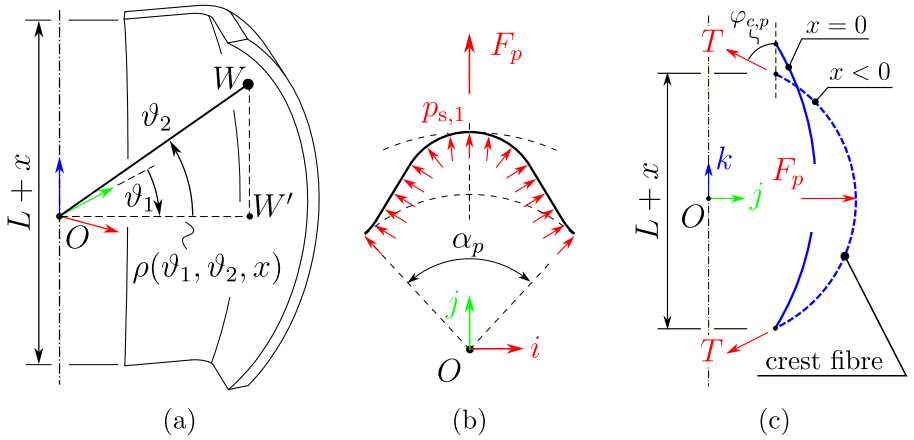



**Fig. 2.** Steps for the evaluation of the pulling force of the actuator.

In a previous work [1], the authors derived an analytical model to estimate the static apply of the actuator. Herein, the model will be briefly presented and then exploited for the computation of air consumption.

Let consider the pulling mode and let the $n$-th pleat of the pleated membrane be defined as a parametric surface (see Fig. 2(a)), that is a function of the two polar coordinates $(\vartheta_1, \vartheta_2)$ and the stroke $x$:

$$\boldsymbol{\Sigma}(\vartheta_1, \vartheta_2, x) = \boldsymbol{OW}(\vartheta_1, \vartheta_2, x) = X\hat{\imath} + Y\hat{\jmath} + Z\hat{k} \tag{1}$$

Therefore, the pressure force $\mathbf{F_p}(x)$ acting on the $n$-th pleat can be evaluated as the surface integral of the pressure distribution $p_{s,1} = P_{s,1} - P_{\text{amb}}$:

$$\mathbf{F_p}(x) = \int_{\Sigma} p_{s,1}\,\hat{n}_1\,d\Sigma = \int_{-\alpha_p/2}^{\alpha_p/2}\int_{-\vartheta_{2,\max}}^{\vartheta_{2,\max}} p_{s,1}\hat{n}_1 \left\| \frac{\partial\boldsymbol{\Sigma}}{\partial\vartheta_1} \times \frac{\partial\boldsymbol{\Sigma}}{\partial\vartheta_2} \right\| d\vartheta_1 d\vartheta_2 \tag{2}$$

where $\hat{n}_1$ is the unit vector that is normal to the surface.

Thanks to the symmetry of the pleat with respect to $\hat{\jmath}$ (see Fig. 2(b)), two components of $\mathbf{F_p}$ are null:

$$\mathbf{F_p} \cdot \hat{k} = \mathbf{F_p} \cdot \hat{\imath} = 0 \tag{3}$$

and the force is purely directed along $\hat{\jmath}$:

$$\mathbf{F_p}(x) = F_p(x)\,\hat{\jmath} \tag{4}$$

Assuming the crest fibres as the main responsible for the load transmission, i.e. that the pressure force $\mathbf{F_p}$ acting on the pleat is entirely balanced by the tension $T$ of the crest fibre (see Fig. 2(c)), then the pulling force $F(x) > 0$ is given by:

$$F(x) = N_p \frac{F_p(x)}{2\,\tan(\varphi_{c,p}(x))} - p_{s,1}A_{\text{a}} + F_{\text{el,b}}(x) + F_{\text{el,p}}(x) \tag{5}$$

The first term in Eq. 5 is the projection of $T$ along $\hat{k}$, and also takes into account the contribution of the $N_p$ pleats. The second term represents the antagonistic force that arises from the pressure acting on the area $A_\mathrm{a}$ between the inner and the outer membranes on the end cap (see Fig. 1(c)). Finally, the latter two terms represent the bellows and the pleated membrane elasticity respectively and can be either evaluated by explicit formulations [7], FEM analysis, or experimentally.

As regards the pushing mode, the calculation of the pushing force $F(x) < 0$ is straightforward:

$$F(x) = -\pi R_{i,b}^2 \, p_{s,2} + F_{\mathrm{el,b}}(x) + F_{\mathrm{el,p}}(x) \tag{6}$$

where $R_{i,b}$ is the bellows radius at the intersection with the end cap, as show in Fig. 1(e).

Let now consider the volume enclosed by the two chambers. Starting from the parametric formulation of the pleated membrane, it can be demonstrated that the volume of chamber 1 is given by:

$$V_1(x) = 2N_p \int_0^{\alpha_p/2} \int_{-\vartheta_{2,\max}}^{\vartheta_{2,\max}} Z(\vartheta_1, \vartheta_2, x)\, \hat{n}_1 \cdot \hat{k} \, d\vartheta_1 d\vartheta_2 + (L + x)\, A_\mathrm{e} - V_2(x) \tag{7}$$

where $A_\mathrm{e}$ is the area of the end cap and $V_2(x)$ is the volume enclosed by chamber 2, which derivation is straightforward and thus omitted.

Equations 5 and 6 can be used to derive the equilibrium condition reached by the actuator in both working conditions. As the deformed configuration of both the bellows and the pleated membrane is known at each stroke $x$, it is thus possible to calculate the volume of the two chambers at the extremes of the range of motion, and finally use this information to estimate the air consumption of the actuator, as it will be illustrated below.

## 3 Characterization of Air Consumption

In this section, the analytical model previously introduced will be exploited to study BiSoft.Q's theoretical air consumption. Then, the air consumption will be experimentally characterized.

### 3.1 Theoretical Estimate

The actuator considered in this study is depicted in Fig. 1(c-d), and its relevant geometrical parameters are listed in Tab. 1. Figure 3(a) shows the static apply obtained with the analytical model at different supply pressures, from which the equilibrium condition for both pulling and pushing phases are derived. It should be noted that the elasticity of the bellows has been included with the same formulation used in [7], while the elasticity of the pleated membrane has been defined as a piece-wise linear polynomial:

$$F_{\mathrm{el,p}}(x) = \begin{cases} \left| N_p \, \dfrac{F_p(x^*_{\min}, p_s)}{2 \tan(\varphi_{c,p})} - p_s A_\mathrm{a} + F_{\mathrm{el,b}}(x^*_{\min}) \right| \cdot \dfrac{x}{x^*_{\min}} & x \le 0 \\ \left| -\pi R_{i,b}^2 \, p_s + F_{\mathrm{el,b}}(x^*_{\max}) \right| \cdot \dfrac{x}{x^*_{\max}} & x > 0 \end{cases} \tag{8}$$

**Table 1.** Relevant geometric parameters of the BiSoft.Q actuator considered in this study.

| | Name | Description | Value | Unit |
|---|---|---|---|---|
| **Pleated membrane** | $L$ | Longitudinal length of the actuator at rest ($x = 0$) | 90 | mm |
| | $l_{c,p}$ | Crest longitudinal arc length | 106 | mm |
| | $R_{oe,p}$ | Radius of the arc defined on the end cap, centered in $O'$ and intersecting the longitudinal crest fibres | 23 | mm |
| | $N_p$ | Number of pleats ($N_p = 2\pi/\alpha_p$) | 8 | - |
| **Bellows** | $R_{i,b}$ | Bellows radius at the intersection with the end cap | 11 | mm |
| | $N_b$ | Number of bellows folds | 5 | - |

where $x^*_{[\text{min,max}]}$ are the strokes measured on the real actuator at a given supply pressure $p_s$. In particular, for a supply pressure $p_s$ = 80 kPa, $x^*_{\text{min}}$ and $x^*_{\text{max}}$ were found to be -16 mm and 5 mm, respectively. Then, these values had been used in Eq. 8 to compute the coefficients of the piece-wise linear approximation of $F_{\text{el,p}}(x)$.

After deriving the equilibrium positions of the actuator from the static apply, it is possible to obtain the corresponding volume of the two chambers. The dead volumes $V_{[1,2],\text{d}}$ and the final volumes $V_{[1,2],\text{f}}$ of the two antagonistic chambers of BiSoft.Q are defined as follows:

$$\begin{cases} V_{1,\text{d}} = V_1(x = x_{\text{max}}), \quad V_{1,\text{f}} = V_1(x = x_{\text{min}}) \\ V_{2,\text{d}} = V_2(x = x_{\text{min}}), \quad V_{2,\text{f}} = V_2(x = x_{\text{max}}) \end{cases} \tag{9}$$

and have been highlighted in Fig. 3(b) for different values of the supply pressure $p_s$.

As regards the computation of air consumption, the mass of air used in the $j$-th chamber to move from one extreme of motion to the other (i.e. from $x_{\text{max}}$ to $x_{\text{min}}$ when chamber 1 is active, and vice versa when chamber 2 is active) is:

$$\Delta M_j = \frac{P_s V_{j,f} - P_{j,i} V_{j,i}}{R T_{\text{amb}}}, \qquad j = 1, 2 \tag{10}$$

where $P_s$ is the absolute supply pressure, $P_{j,i}$ and $V_{j,i}$ are respectively the initial absolute pressure and volume in the $j$-th chamber, $V_{j,f}$ is the final volume of the $j$-th chamber, $R$ is the specific gas constant of air and $T_{\text{amb}}$ is the ambient temperature. In Eq. 10 an isothermal transformation has been implicitly assumed. The final volume $V_{j,f}$ can be rewritten as:

$$V_{j,f} = V_{j,i} + \Delta V_j \tag{11}$$

As the $j$-th chamber is connected to atmosphere before activation and its initial volume represents a dead volume (i.e. $V_{j,i} = V_{j,d}$), Eq. 10 can be rewritten in the following way:

$$\Delta M_j = \frac{(P_s - P_{\text{amb}})\, V_{j,d}}{R T_{\text{amb}}} + \frac{P_s \Delta V_j}{R T_{\text{amb}}}, \qquad j = 1, 2 \tag{12}$$

In Eq. 12 the first term represents the mass of air needed to pressurize the dead volume $V_{j,d}$ from $P_{\text{amb}}$ to $P_s$. The contribution of this term on air consumption corresponds

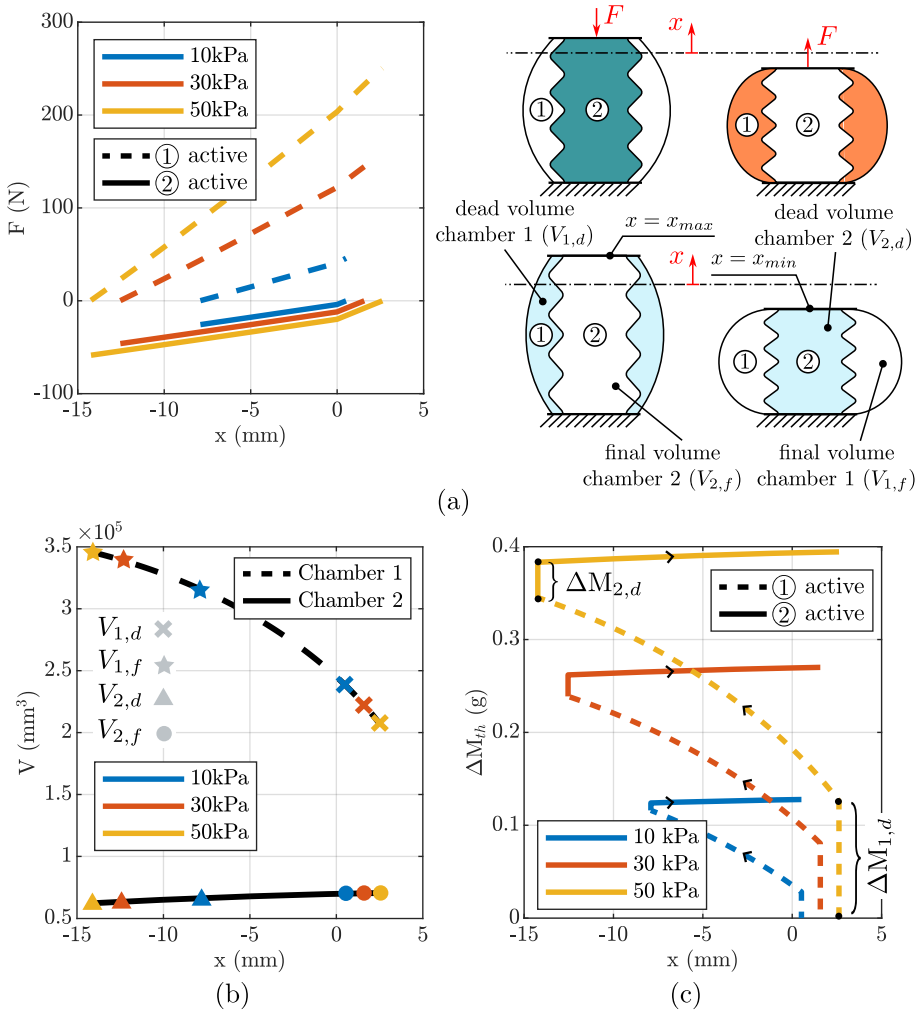



**Fig. 3.** (a) Static apply derived from the analytical model at different supply pressures. (b) Volume of the antagonistic chambers as a function of stroke $x$. The dead volumes $V_{[1,2],\mathrm{d}}$ and the final volumes $V_{[1,2],\mathrm{f}}$ of the two chambers have been highlighted for different supply pressures. (c) Theoretical air consumption of BiSoft.Q at different supply pressures, evaluated starting from the fully elongated configuration $x = x_{\max}$ and performing a complete actuation cycle. $\Delta M_{1,d}$ and $\Delta M_{2,d}$ are the masses of air needed to pressurize the dead volumes of the chambers.

to the vertical jumps that are observed in Fig. 3(c). Finally, the mass of air used in a complete actuation cycle is given by:

$$\Delta M = \Delta M_1 + \Delta M_2 \tag{13}$$

The formulation adopted neglects the dynamics of the actuator's chambers filling and discharging, effectively assuming instantaneous pressure transitions. The active chamber's gauge pressure is modeled as instantaneously rising from zero to the supply pressure ($p_s$), while in the other chamber, the gauge pressure instantaneously drops to zero. While deviating from real-world behavior, this simplification provides a readily estimate of air consumption, particularly useful during the design phase when comparing different geometries. Once the geometry has been defined, a more comprehensive dynamic model incorporating the actuator and its pneumatic supply can refine the air consumption prediction.

### 3.2 Experimental Characterization

The experimental setup used for the characterization of the BiSoft.Q's air consumption is visible in Fig. 4. The actuator was connected to a rigid reservoir with a volume of 3.8 liters by means of two 3/2 solenoid valves. The pressure in the reservoir and in the proximity of the actuator's chambers was measured by pressure transducers with a full scale of 207 kPa and an accuracy of 0.25%. Moreover, the linear motion of the actuator was measured through a linear potentiometer. The tests were conducted by first pressurizing the reservoir and then performing a number of actuation cycles until complete discharge. During each cycle, a sufficient amount of time was given before switching the solenoid valves, in order to reach a stationary condition. Finally, the air consumption was derived indirectly by monitoring the pressure inside the reservoir. Experimental data from a representative test are shown in Fig. 5.

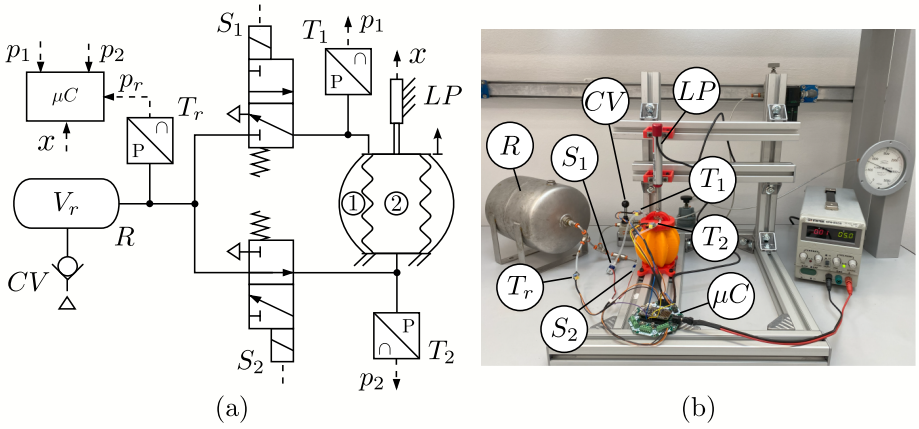



**Fig. 4.** Experimental setup used for the characterization of BiSoft.Q's air consumption.

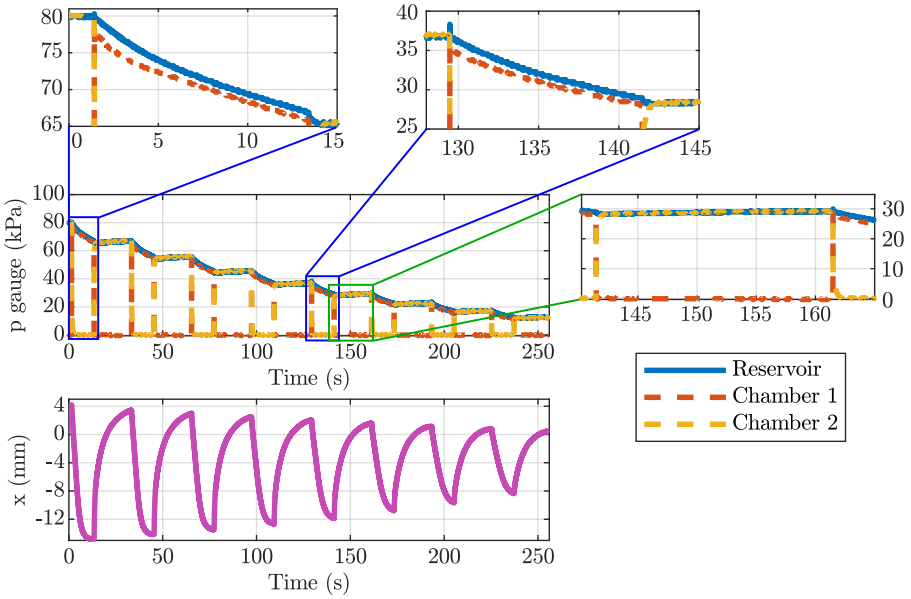



**Fig. 5.** Experimental data acquired during a test. When chamber 1 is active, air leakages to the atmosphere cause the pressure in chamber 1 to be lower than the reservoir pressure.

## 4 Results

The comparison between the theoretical and experimental results can be found in Fig. 6. The theoretical air consumption is slightly smaller than the real one, with an average difference of about -8%. In detail, the discrepancy increases as the supply pressure increases. The reasons for this behavior are to be identified in:

- minor leakages in the deformable membranes, which have been considerably limited, but not eliminated, by applying a liquid latex sealant. As shown in Fig. 5, leakages caused the pressure in chamber 1 to be lower than the reservoir pressure, and that effect was accentuated at higher pressures;
- ballooning of the pleated membrane that manifests as a deformation in the radial direction mainly at the valley fibers, which does not correspond to a significant longitudinal contraction. This results in an effective final volume of the outer chamber bigger than the one computed analytically.

Among the aforementioned aspects, leakages represent the most significant factor affecting the reliability of the proposed model, due to the difficulty in controlling them.

As regards the actuation strokes, the ones predicted by the model and the experimental ones show good accordance: this means that the static apply model, integrated with the piece-wise linear approximation of the elastic force of the pleated membrane (Eq. 8), can be successfully used to estimate the actuation strokes of the actuator.

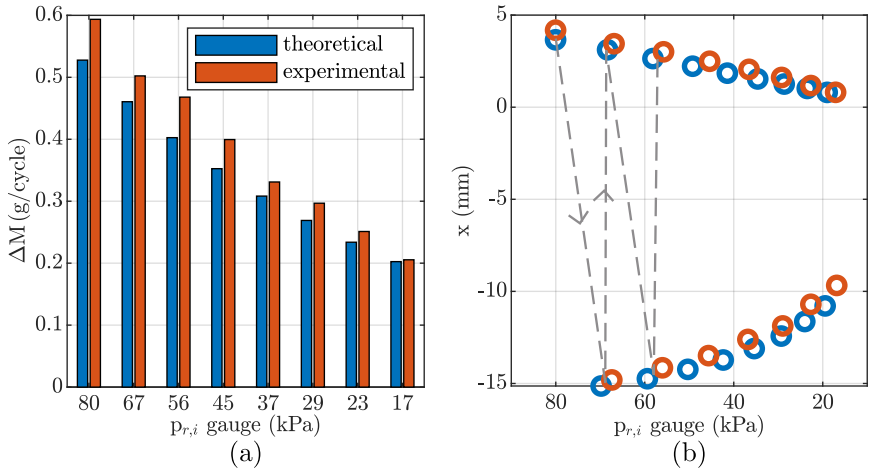



**Fig. 6.** Comparison between theoretical and experimental results: (a) air consumption, (b) equilibrium positions, at different initial gauge pressures $p_{\mathrm{r,i}}$ in the reservoir. The gray arrows show in which direction the actuation cycles were performed.

## 5 Conclusions

This paper presented a theoretical model to estimate the air consumption of a bidirectional Soft Pneumatic Actuator. An analytical method for the computation of the actuation forces is used to estimate the equilibrium condition reached by the actuator for a given supply pressure. This information is then used to find the volume of the two chambers, and finally the mass of air required to reach the equilibrium condition. Moreover, an experimental characterization of the air consumption of the actuator was performed and the model was validated.

Future work will involve analyzing and implementing strategies to reduce air consumption, such as internal exhaust air recirculation between the chambers and filling with granular or liquid media. Another possible area of study includes developing a dynamic model to estimate the actuator's dynamic performance for each of the energy-saving strategies that will be implemented.

## Acknowledgments

The present work was conducted in the framework of the TWIN-IT-ROMANS project (https://twin-it-romans.iyte.edu.tr/), titled "Twinning IzTech in Robotics Manufacturing Systems," which has received funding from the European Union's Horizon Europe Framework Programme HORIZON-WIDERA-2023-ACCESS-02 (Twinning Bottom-Up) under Grant Agreement No 101160215.

## References

1. Colucci, G., Duretto, S., Quaglia, G.: Design and Prototyping of BiSoft.Q, A 3-D Printed Bi-directional Deformable Actuator. In: Advances in Mechanism and Machine Science. pp. 710–720. Springer Nature Switzerland (2024)
2. Daerden, F., Lefeber, D.: The Concept and Design of Pleated Pneumatic Artificial Muscles. International Journal of Fluid Power **2**(3), 41–50 (2001)
3. Davis, S., Canderle, J., Artrit, P., Tsagarakis, N., Caldwell, D.: Enhanced dynamic performance in pneumatic muscle actuators. In: Proceedings 2002 IEEE International Conference on Robotics and Automation. vol. 3, pp. 2836–2841 vol.3 (2002)
4. Feng, M., Yang, D., Majidi, C., Gu, G.: High-Speed and Low-Energy Actuation for Pneumatic Soft Robots with Internal Exhaust Air Recirculation. Advanced Intelligent Systems **5**(4), 2200257 (2023)
5. Focchi, M., Guglielmino, E., Semini, C., Parmiggiani, A., Tsagarakis, N., Vanderborght, B., Caldwell, D.G.: Water/air performance analysis of a fluidic muscle. In: 2010 IEEE/RSJ International Conference on Intelligent Robots and Systems. pp. 2194–2199 (2010)
6. Lee, S., Lee, D., Shin, D.: An Air Recirculation System Based on Bioinspired Soft Re-Air Valve for Highly Efficient Pneumatic Actuation. Soft Robotics **8**(5), 564–576 (2021)
7. Wang, Z., Hirata, T., Sato, T., Mori, T., Kawakami, M., Furukawa, H., Kawamura, S.: A Soft Robotic Hand Based on Bellows Actuators for Dishwashing Automation. IEEE Robotics and Automation Letters **6**(2), 2139–2146 (2021)